FIGURE S1

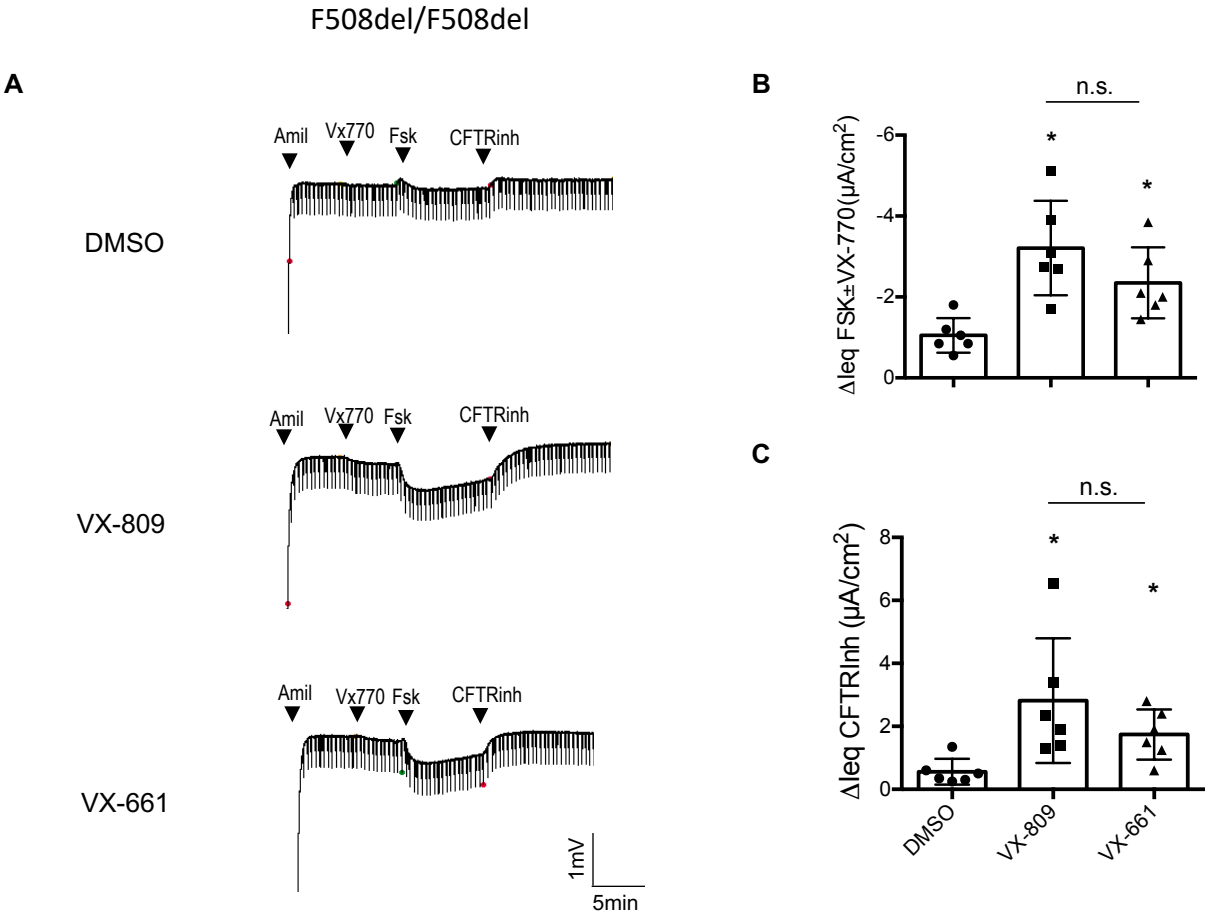
F508del/F508del
A
Amil
Vx770
Fsk
CFTRinh
DMSO
VX-809
VX-661
1mV
5min
B
n.s.
ΔIeq FSK±VX-770(μA/cm²)
-6
-4
-2
0
C
n.s.
ΔIeq CFTRInh (μA/cm²)
8
6
4
2
0
DMSO
VX-809
VX-661

FIGURE S1: ORKAMBI and SYMDEKO showed similar rescue of F508del-CFTR in nasal epithelial cultures derived from 6 patients homozygous for F508del/F508del. (**A**) Representative tracing show Ussing chamber studies measurements of CFTR function in nasal epithelial cell cultures from F508del/F508del patients after pre-treatment with DMSO, VX-809 (3 μM) or VX-661 (3 μM). (**B**) Bar graphs showing the mean (±SD) of maximal response Ieq ($\mu A/cm^2$) after stimulation with forskolin (10 μM) + VX-770 (l μM) (2 inserts for each treatment). (**C**) Bar graphs showing the $IeqCFTR_{inh-172}$ ($\mu A/cm^2$) by $CFTR_{Inh-172}$ (10 μM). Comparative analysis was performed using by one-way ANOVA followed by Turkey's post-hoc test. *$p<0.05$.

FIGURE S2

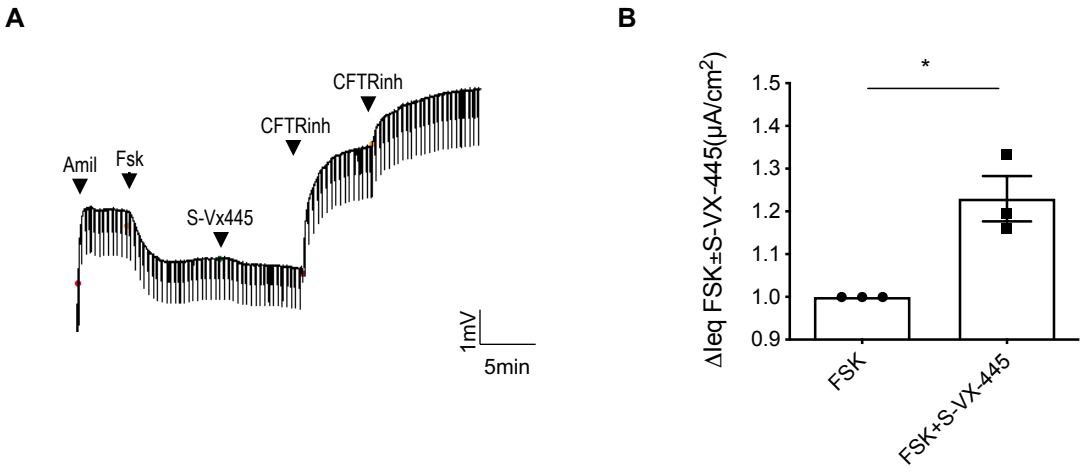
A
Amil
Fsk
S-Vx445
CFTRinh
CFTRinh
1mV
5min
B
*
ΔIeq FSK±S-VX-445(μA/cm²)
1.5
1.4
1.3
1.2
1.1
1.0
0.9
FSK
FSK+S-VX-445

FIGURE S2: VX-445 compound increased channel activation of Wt-CFTR in nasal epithelial cells. (A) Representative trace showing Ussing chamber measurements of CFTR function in nasal epithelial cell cultures from a non-CF donor. (**B**) Bar graphs showing the fold increased forskolin (0.1 µM) + [S]-VX-445 (3 µM) activated ΔIeq compared to forskolin (0.1 µM) control in 3 technical replicated nasal epithelial cells generated from 1 healthy control. *$p<0.05$.

FIGURE S3

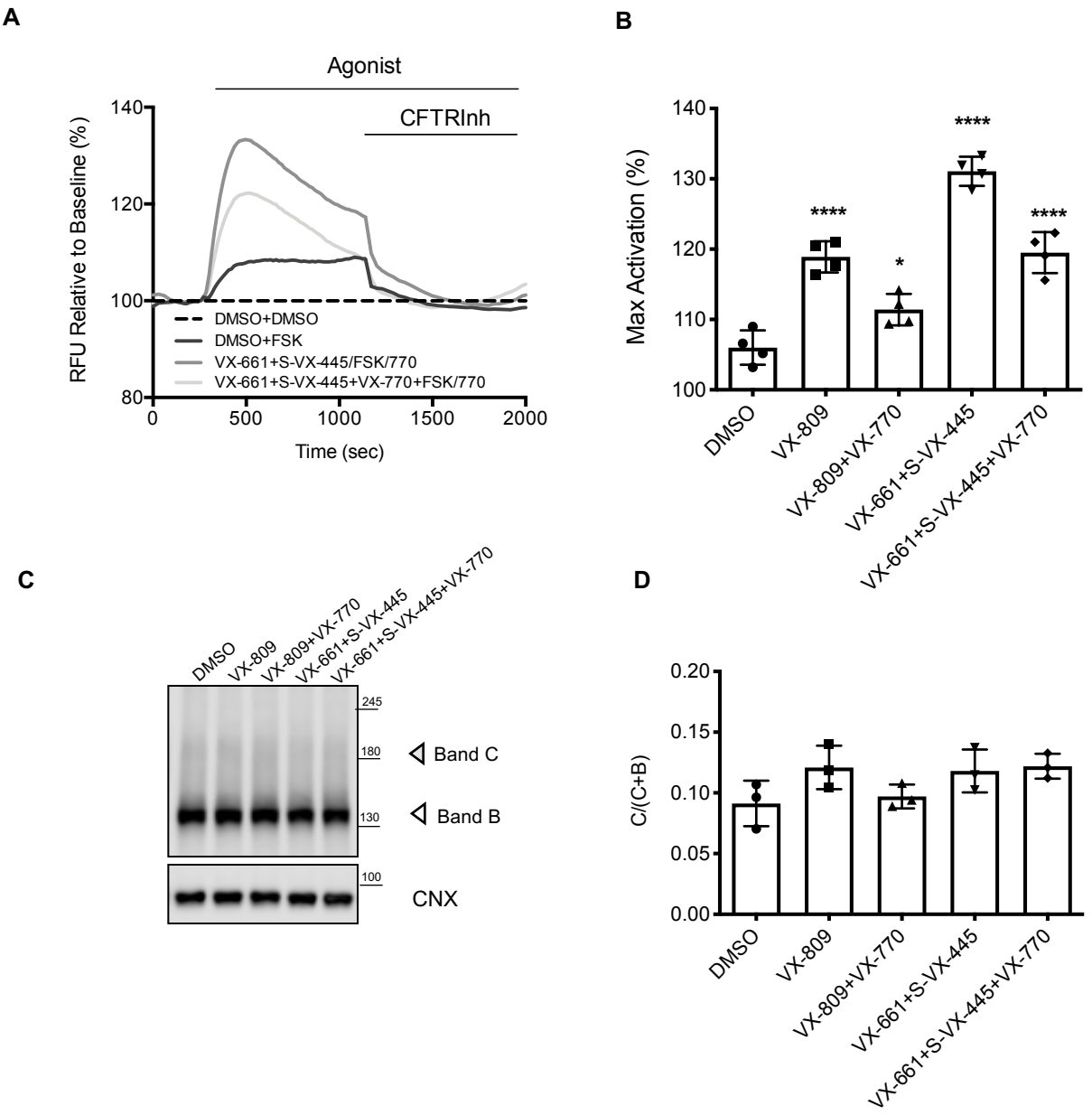
A
Agonist
CFTRInh
RFU Relative to Baseline (%)
140
120
100
80
0
500
1000
1500
2000
Time (sec)
DMSO+DMSO
DMSO+FSK
VX-661+S-VX-445/FSK/770
VX-661+S-VX-445+VX-770+FSK/770
B
Max Activation (%)
140
130
120
110
100
****
*
****
****
DMSO
VX-809
VX-809+VX-770
VX-661+S-VX-445
VX-661+S-VX-445+VX-770
C
DMSO
VX-809
VX-809+VX-770
VX-661+S-VX-445
VX-661+S-VX-445+VX-770
245
180
130
100
Band C
Band B
CNX
D
C/(C+B)
0.20
0.15
0.10
0.05
0.00
DMSO
VX-809
VX-809+VX-770
VX-661+S-VX-445
VX-661+S-VX-445+VX-770

FIGURE S3: VX-445+ VX-661+ VX-770 showed functional rescue of N1303K-CFTR in CFF 16HBEge CFTR-N1303K. (A) Representative traces of N1303K-CFTR-dependent chloride efflux by FLIPR assay in HBE cells pre-treated with DMSO, VX-809 (3 µM), [S]-VX-445 (3 µM)+ VX-661 (3 µM), VX-661 (3 µM)+ VX-770 (1 µM) or [S]-VX-445 (3 µM)+ VX-661 (3 µM)+ VX-770 (1 µM) for 24 hrs at 37°C. (**B**) Bar graphs show the mean (±SD) of maximal activation of N1303K-CFTR after stimulation by FSK (10 µM) +/- VX-770 (1 µM) (n= 4 biological replicates and 4 technical replicates for each experiment) *$p<0.05$; ****$p<0.0001$ by one way ANOVA followed by Turkey's post-hoc test.

FIGURE S4

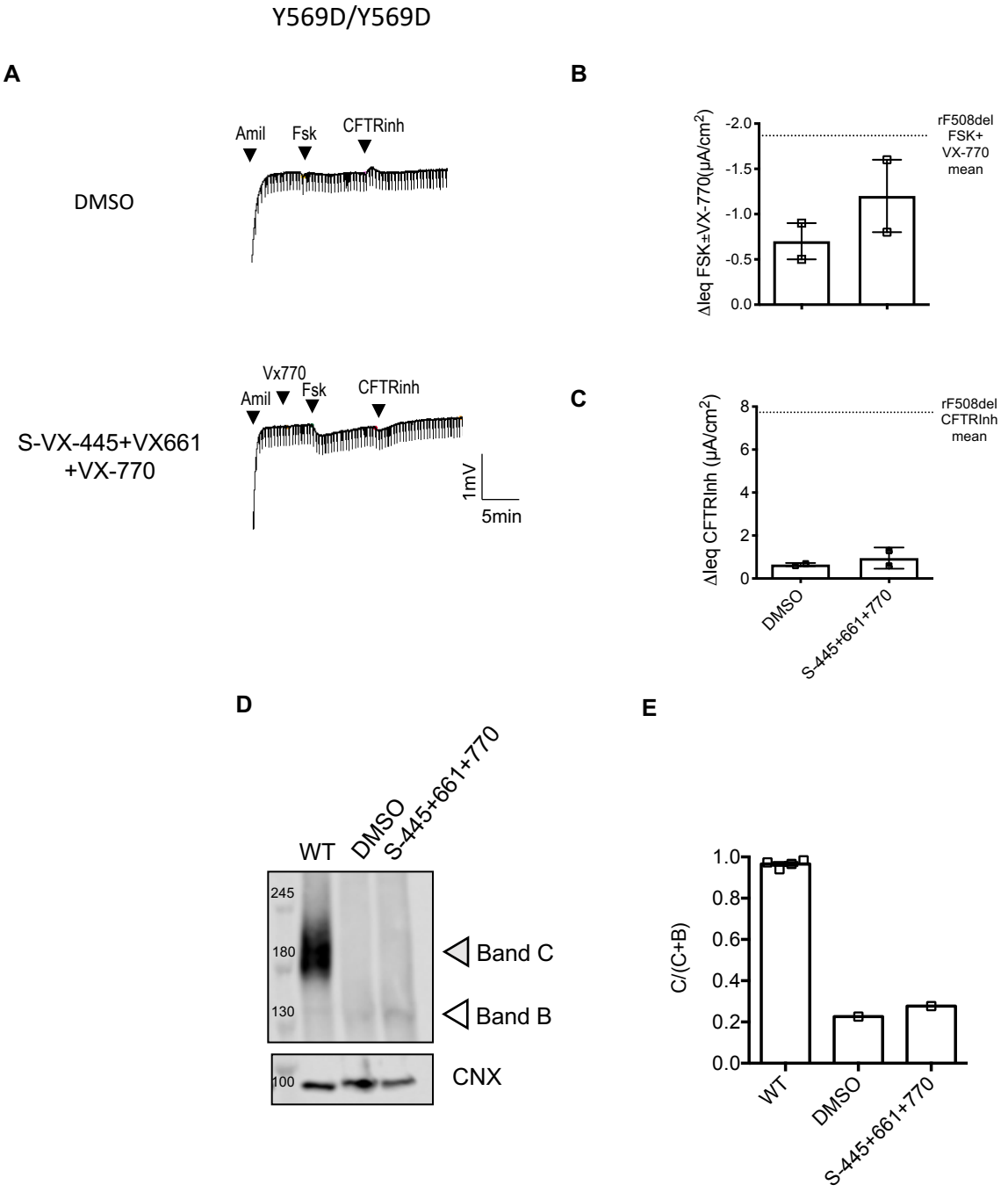
Y569D/Y569D
A
DMSO
Amil
Fsk
CFTRinh
S-VX-445+VX661
+VX-770
Vx770
1mV
5min
B
ΔIeq FSK±VX-770(μA/cm²)
rF508del
FSK+
VX-770
mean
C
ΔIeq CFTRInh (μA/cm²)
rF508del
CFTRInh
mean
DMSO
S-445+661+770
D
WT
DMSO
S-445+661+770
245
180
130
Band C
Band B
100
CNX
E
C/(C+B)
WT
DMSO
S-445+661+770

FIGURE S4: VX-445+ VX-661+ VX-770 failed to rescue Y569D-CFTR channel activity in nasal epithelial cultures derived from 1 patient homozygous for Y569D/Y569D. (A) Representative tracings show Ussing chamber measurements of CFTR function in nasal epithelial cell cultures from 1 CF patient bearing Y596D/Y569D in the absence or presence of the [S]-VX-445+ VX-661+ VX-770. (**B**) Bar graphs showing the mean (±SD) of maximal response Ieq ($\mu A/cm^2$) after stimulation by forskolin (10 µM) +/- VX-770 (l µM) for nasal cultures from 1 patient bearing Y596D/Y569D after pre-treatment (48 hrs at 37°C) with DMSO (0.1%) or [S]-VX-445 (3 µM)+ VX-661 (3 µM)+ VX-770 (1 µM) (2 inserts for each treatment). (**C**) Bar graphs showing the IeqCFTR inhibition ($\mu A/cm^2$) by $CFTR_{Inh\text{-}172}$ (10 µM) (2 inserts for each treatment). (**D**) Immunoblots of steady-state expression of Wt or Y596D/Y569D following treatments with CFTR modulators. Band C: mature, complex-glycosylated CFTR; Band B: immature, core-glycosylated CFTR; CNX: Calnexin. (**E**) Bars represent the ratio of band C/(band C+ band B) (n=2). Statistical analysis was performed using paired two-tailed Student's t-test.

FIGURE S5

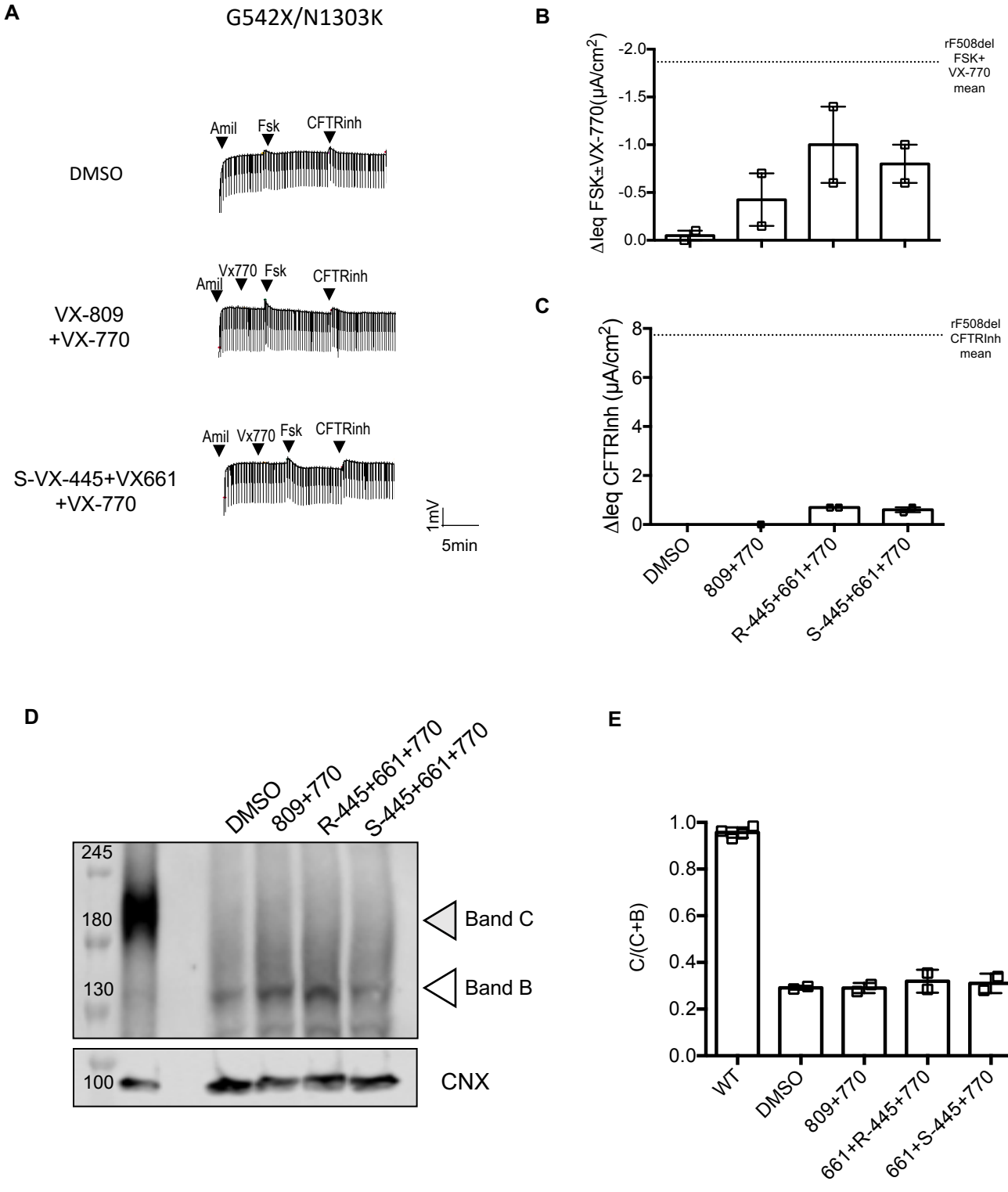
A
G542X/N1303K
DMSO
Amil
Fsk
CFTRinh
VX-809
+VX-770
Vx770
S-VX-445+VX661
+VX-770
1mV
5min
B
ΔIeq FSK±VX-770(μA/cm²)
rF508del
FSK+
VX-770
mean
C
ΔIeq CFTRInh (μA/cm²)
rF508del
CFTRInh
mean
DMSO
809+770
R-445+661+770
S-445+661+770
D
245
180
130
100
Band C
Band B
CNX
E
C/(C+B)
WT
661+R-445+770
661+S-445+770

FIGURE S5: VX-445+ VX-661+ VX-770 showed minimal increase in CFTR activity in nasal epithelial cultures derived from patients with G542X/N1303K mutation (n=2). (A) Representative tracings show Ussing chamber measurements of CFTR function in nasal epithelial cell cultures from a CF patient bearing G542X/N1303K in the absence or presence of the small molecule corrector. (**B**) Bar graphs showing the mean (±SD) of maximal response Ieq ($\mu A/cm^2$) after stimulation by forskolin (10 µM) +/- VX-770 (l µM) of 1-2 technical replicates of nasal epithelial cell cultures generated from 2 patients bearing G542X/N1303K. Nasal epithelial cells were treated (48h at 37°C) with DMSO (0.1%), VX-809 (3 µM)+ VX-770 (1 µM), R-VX-445 (3 µM)+ VX-661 (3 µM)+ VX-770 (1 µM) or [S]-VX-445 (3 µM)+ VX-661 (3 µM)+ VX-770 (1 µM) (2-3 inserts for each treatment). (**C**) Bar graphs showing the mean (±SD) $IeqCFTR_{inh-172}$ ($\mu A/cm^2$) by $CFTR_{Inh-172}$ (10 µM). (**D**) Immunoblots of steady-state expression of G542X/N1303K following treatments with CFTR modulators. Band C: mature, complex-glycosylated CFTR; Band B: immature, core-glycosylated CFTR; CNX: Calnexin. (**E**) Bars represent the mean (±SD) of the ratio band C/(band C+ band B) (n=2). Statistical analysis was performed using one-way ANOVA followed by Turkey's post-hoc test.